Continental Shelf Research 28 (2008) 1273–1285

Contents lists available at ScienceDirect

Continental Shelf Research

journal homepage: www.elsevier.com/locate/csr

Statistical models for sediment/detritus and dissolved absorption coefficients in coastal waters of the northern Gulf of Mexico

Rebecca E. Green [a,*], Richard W. Gould Jr.[a,1], Dong S. Ko [b,2]

[a] Ocean Optics Section, Code 7333, Naval Research Laboratory, Stennis Space Center, MS 39529, USA
[b] Coastal and Semi-Enclosed Seas Section, Code 7322, Naval Research Laboratory, Stennis Space Center, MS 39529, USA

ARTICLE INFO

Article history:
Received 30 July 2007
Received in revised form
23 January 2008
Accepted 25 February 2008
Available online 13 March 2008

Keywords:
Coastal waters
River plume
Optical properties
CDOM
Tripton
Satellite

ABSTRACT

We developed statistically-based, optical models to estimate tripton (sediment/detrital) and colored dissolved organic matter (CDOM) absorption coefficients (a_{sd}, a_g) from physical hydrographic and atmospheric properties. The models were developed for northern Gulf of Mexico shelf waters using multi-year satellite and physical data. First, empirical algorithms for satellite-derived a_{sd} and a_g were developed, based on comparison with a large data set of cruise measurements from northern Gulf shelf waters; these algorithms were then applied to a time series of ocean color (SeaWiFS) satellite imagery for 2002–2005. Unique seasonal timing was observed in satellite-derived optical properties, with a_{sd} peaking most often in fall/winter on the shelf, in contrast to summertime peaks observed in a_g. Next, the satellite-derived values were coupled with the physical data to form multiple regression models. A suite of physical forcing variables were tested for inclusion in the models: discharge from the Mississippi River and Mobile Bay, Alabama; gridded fields for winds, precipitation, solar radiation, sea surface temperature and height (SST, SSH); and modeled surface salinity and currents (Navy Coastal Ocean Model, NCOM). For satellite-derived a_{sd} and a_g time series (2002–2004), correlation and stepwise regression analyses revealed the most important physical forcing variables. Over our region of interest, the best predictors of tripton absorption were wind speed, river discharge, and SST, whereas dissolved absorption was best predicted by east–west wind speed, river discharge, and river discharge lagged by 1 month. These results suggest the importance of vertical mixing (as a function of winds and thermal stratification) in controlling a_{sd} distribution patterns over large regions of the shelf, in comparison to advection as the most important control on a_g. The multiple linear regression models for estimating a_{sd} and a_g were applied on a pixel-by-pixel basis and results were compared to monthly SeaWiFS composite imagery. The models performed well in resolving seasonal and interannual optical variability in model development years (2002–2004) (mean error of 32% for a_{sd} and 29% for a_g) and in predicting shelfwide optical patterns in a year independent of model development (2005; mean error of 41% for a_{sd} and 46% for a_g). The models provide insight into the dominant processes controlling optical distributions in this region, and they can be used to predict the optical fields from the physical properties at monthly timescales.

1. Introduction

As a dynamic river-dominated margin, northern Gulf of Mexico shelf waters play a significant role in mediating the large flux of terrestrial materials from north America into coastal and deep ocean waters. The Mississippi River is the seventh largest in the world by freshwater and sediment flux, and drains a vast region (41%) of the continental United States (van der Leeden et al. 1990). High concentrations of dissolved nitrate from the river ($>100\,\mu mol\,L^{-1}$; Dagg and Whitledge, 1991) support significant phytoplankton growth on the shelf (e.g., Lohrenz et al., 1999) and one of the United States' most productive fisheries. Over the last 50 years, high primary production due to increased riverborne nutrients is considered responsible for the large zone of summertime hypoxia that forms on the Louisiana–Texas shelf, currently the second largest zone of coastal hypoxia in the world (Rabalais et al., 2002). In addition to nutrient availability, phytoplankton growth on the shelf is also strongly controlled by light availability (e.g., Lohrenz et al., 1999), as large inputs of suspended sediments and dissolved materials enter the shelf from a variety of sources and attenuate light. The Mississippi River alone delivers 2.0×10^{11} kg of suspended sediments and

* Corresponding author. Tel.: +1 228 688 5576; fax: +1 228 688 4149.
E-mail addresses: rgreen@nrlssc.navy.mil (R.E. Green), rgould@nrlssc.navy.mil (R.W. Gould Jr.), ko@nrlssc.navy.mil (D.S. Ko).
[1] Tel.: +1 228 688 5587; fax: +1 228 688 4149.
[2] Tel.: +1 228 688 5448; fax: +1 228 688 4149.

0278-4343/$ - see front matter © 2008 Elsevier Ltd. All rights reserved.
doi:10.1016/j.csr.2008.02.019

3.1×10^9 kg of dissolved organic carbon (DOC) to the Louisiana shelf annually (Meade, 1996; Bianchi et al., 2004). The coastal zone of Louisiana contains ~41% of the nation's coastal wetlands, and these regions are also sources of terrestrial organic matter to the shelf (e.g., Engelhaupt and Bianchi, 2001), in addition to numerous smaller rivers.

An improved understanding of the environmental controls on dissolved and suspended particulate materials (including detritus and sediments) on the shelf is requisite to our understanding of light limitation on phytoplankton growth, as well as to the overall cycling of terrestrial materials introduced from rivers and shallow coastal environments. A variety of biological and physical mechanisms can impact sediment/detrital and dissolved distributions in surface waters of the northern Gulf of Mexico. Physical mixing of freshwater inputs and high salinity Gulf waters strongly influences surface property distributions, with both particulate and dissolved concentrations generally decreasing in the offshore direction away from riverine sources (e.g., Trefry et al., 1992; Benner and Opsahl, 2001). Seasonal variability in river discharge and wind speed also affects surface property distributions. For example, time series analyses of satellite-derived suspended particulate matter (SPM) concentrations on the shelf demonstrated strong positive correlations with both river discharge and wind speed (Walker, 1996; Salisbury et al., 2004). In some shelf regions, increased wind speeds can lead to particle resuspension and seaward transport, resulting in increased particulate concentrations in surface waters (e.g., Walker and Hammack, 2000). Fluorescence measurements have shown that several factors control colored dissolved organic matter (CDOM) distributions on the shelf. At short time scales (daily), CDOM concentrations appear to be largely controlled by conservative mixing between freshwater and marine endmembers, with inputs from both rivers and coastal wetlands (Hitchcock et al., 2004). Significant in situ biological input of CDOM has also been observed, along with some evidence of flocculation and minor photobleaching effects (Chen et al., 2004). Certainly numerous other factors will likely contribute to particulate and dissolved matter variability on the shelf, including physico-chemical processes such as aggregation and desorption, as well as biological uptake and release processes related to microbial transformations, primary production, and grazing (for review, see Dagg et al., 2004).

Satellite remote sensing can provide the synoptic data to study surface ocean constituents at high spatial and temporal resolution, even in coastal waters. Previously, in situ cruise measurements have shown significant spatial and temporal variability in detrital and CDOM absorption in the Louisiana Bight (D'Sa et al., 2006). However, while cruise measurements are necessary for algorithm development, especially in coastal regions, satellite measurements can allow for higher temporal resolution time series analyses and for larger spatial coverage. SPM distributions have been the focus of several satellite-based studies in the northern Gulf (e.g., Walker, 1996; Salisbury et al., 2004), but there have been no similar studies of satellite-derived tripton (non-algal particle) and CDOM distributions in this region. Traditionally, ocean color remote sensing algorithms have allowed for the retrieval of total absorption and backscattering coefficients, with the further separation of total absorption into a phytoplankton and combined CDOM/tripton component (Lee et al., 2002; Maritorena et al., 2002). An expanding data set of optical measurements for northern Gulf shelf waters (e.g., D'Sa et al., 2007; Green and Gould, 2008) sets the stage for the development of regional algorithms for CDOM and tripton absorption in this paper. As well, improved techniques for processing satellite imagery in coastal regions have been developed. These include more accurate methods for atmospheric correction of satellite imagery, such as a near-infrared correction scheme for estimating water-leaving radiance at 670 nm (Arnone et al., 1998; Stumpf et al., 2003), as well as a new absorbing aerosol correction (Ransibrahmanakul and Stumpf, 2006).

In this study, our goal was to develop satellite algorithms for estimating tripton and CDOM absorption in the northern Gulf of Mexico and to apply these to development of statistically-based, predictive models for both absorption components. Predictive optical models represent an important avenue of current research in the oceanic sciences, with applications ranging from forecasting light fields for phytoplankton growth to predicting underwater visibility for naval and maritime operations (e.g., Dickey et al., 2006). Previously, we developed a predictive model for satellite-derived phytoplankton variability in Louisiana shelf waters using a host of environmental forcing mechanisms (Green and Gould, 2008). In the current study, we expanded our region-of-interest to include a larger portion of the northern Gulf (Louisiana, Mississippi, and Alabama coastal waters), and updated our physical forcing database to include several forcing fields of higher spatial resolution (e.g., winds, precipitation, and surface salinity and currents). We first develop empirical algorithms for estimating CDOM and sediment/detrital absorption coefficients (a_g, a_{sd}) from satellite measurements, and then use our algorithms to describe multi-year, satellite-derived optical variability in shelf waters. Secondly, we develop statistically based models for both a_g and a_{sd} for mean monthly imagery from 2002 to 2004 and demonstrate the predictive capability of the models in application to 2005.

2. Methods

2.1. Cruise measurements

Measurements of optical properties were made in northern Gulf of Mexico coastal waters during seven field experiments. Measurements were obtained during two cruises on the Louisiana shelf aboard the R/V *Pelican* (27 April–1 May 2006) and OSV *Bold* (6–11 September 2006). Surface water samples were collected using a conductivity–temperature–depth profiler/rosette system equipped with sampling bottles. All samples were processed onboard ship within 2–3 h of sample collection. As well, two nearshore samplings in shallower waters of the Louisiana shelf were conducted as transects out of Vermilion, Terrebonne, and Barataria Bays (17–19 May and 17–19 July 2007). Three field experiments were also conducted off the Mississippi/Alabama coasts during 20–24 May 2002, 13 December 2005, and 6 February 2007. During these experiments, samples were collected on day trips and processed that evening or the next day onshore. Sample sites were generally located inside the 50 m isobath, with the majority of stations within the 15 m isobath (Fig. 1).

Absorption coefficients for particulate material (a_p) and CDOM (a_g) in surface water samples were measured spectrophotometrically. Particulate material was collected on GF/F filters (nominal pore size of 0.7 μm), and absorption coefficients were measured using an analytical spectral devices (ASD) fiber optic-based spectrophotometer. Subsequent to the initial optical density measurements for particulates, filters were extracted for 20 min in hot methanol (to remove phytoplankton pigments) and reanalyzed to determine the residual particulate absorption by sediment and detritus (a_{sd}) (Kishino et al., 1985). We here use the subscript "sd" in a_{sd} to refer to the sum of absorption by inorganic suspended sediments and organic detritus. We will also refer to this non-living particulate pool composed of both sediments and detritus as "tripton". All particulate measurements were relative to a blank filter saturated with milli-Q water, and the optical density (OD) at 850 nm for the blank was subtracted from each

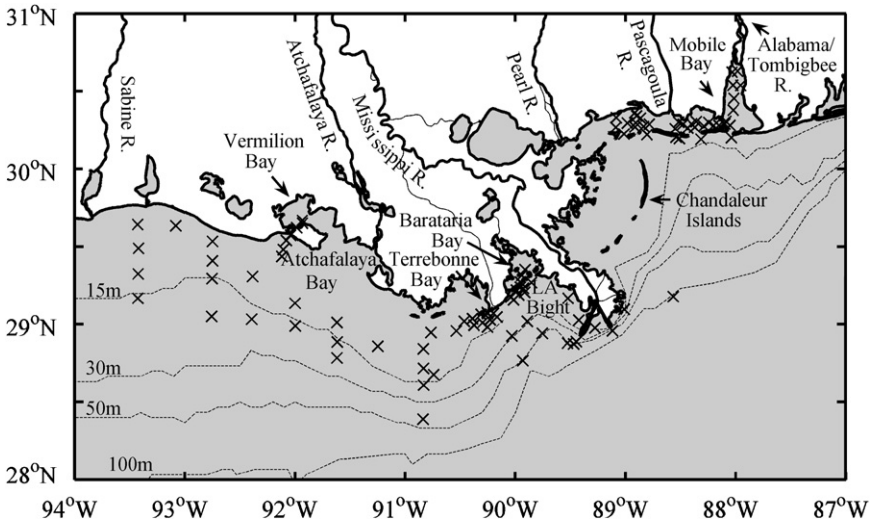

Fig. 1. Map of study region in the northern Gulf of Mexico, including the Louisiana, Mississippi, and western Alabama coastlines. Locations of sample sites for all seven field experiments are indicated (×).

sample spectrum. A path length amplification (β) factor was used to correct optical density measurements for particle concentration and filter effects; this factor was determined specifically for our ASD spectrophotometer, as described in Green and Gould, 2008). Absorption by CDOM (a_g) was measured on the GF/F filtrate, also using the ASD spectrophotometer. Measurements were made in a 10-cm quartz cuvette, referenced to a milli-Q blank, and corrected for baseline offsets by subtracting average absorption from each spectrum between 690 and 700 nm. A set of 122 absorption spectra were obtained in all.

2.2. Remote sensing algorithms

Data from the Sea-viewing Wide-Field-of-View Sensor (SeaWiFS) were collected, processed, and archived for the Gulf of Mexico. The 1 km-resolution imagery was processed with the Naval Research Laboratory's Automated Processing System (APS) (Martinolich, 2005). APS Version 3.5 utilized atmospheric correction algorithms proscribed by NASA's fifth SeaWiFS reprocessing, and includes a near-infrared (NIR) correction for coastal waters (Arnone et al., 1998; Stumpf et al., 2003). The NIR atmospheric correction method used by APS improves estimates of bio-optical parameters in coastal regions by applying an iterative technique in which water-leaving radiance at 765 and 865 nm is estimated from water-leaving radiance at 670 nm. An absorbing aerosol correction was also applied to improve underestimates of satellite-derived water reflectance (Ransibrahmanakul and Stumpf, 2006). In our time series analyses, we used monthly composite imagery for 2002–2005, which were temporal averages of all valid pixels (e.g., cloud-free) in each month.

Algorithms for deriving total, tripton, and CDOM absorption from satellite measurements were developed and validated. Satellite-derived total absorption ($a_t(443)$) and backscattering ($b_b(555)$) coefficients were obtained from an updated version of the quasi-analytical algorithm (QAA, v.4) of Lee et al. (2002; 2007). In the QAA model, absorption and backscattering coefficients are analytically calculated from spectral values of remote sensing reflectance (R_{rs}). The updated QAA model achieves a more seamless transition from open ocean to coastal waters. Previous work has shown that non-living organic and mineral particles are the primary contributors to b_b (e.g., Stramski and Kiefer, 1991; Green et al., 2003), and recent cruise measurements have shown a strong relationship between b_b and non-algal particle absorption on the Louisiana shelf (D'Sa et al., 2007). Thus, we compared both satellite-derived $a_t(443)$ and $b_b(555)$ values to our measured values of $a_t(443)$ and $a_{sd}(443)$, respectively, to derive our final satellite-based algorithms for these absorption coefficients (see Section 3). Total absorption is the sum of absorption by all seawater constituents, including absorption by pure seawater (a_w), tripton (a_{sd}), phytoplankton (a_{ph}), and CDOM (a_g). Hence, we calculated absorption by CDOM as the difference between total absorption and each seawater constituent as follows:

$$a_g = a_t - a_w - a_{sd} - a_{ph}, \tag{1}$$

where $a_w \approx 7.07 \times 10^{-3}$ at 443 nm (Pope and Fry, 1997). We calculated phytoplankton absorption from satellite-derived chlorophyll (Chl; Stumpf et al., 2000), using the following algorithm of Green and Gould, 2008:

$$\log_{10}(a_{ph}) = 0.847 Chl^{0.361} - 2.03. \tag{2}$$

This a_{ph} algorithm was determined based on comparison with numerous cruise measurements from northern Gulf of Mexico coastal waters. The Stumpf chlorophyll product is an empirical algorithm that was developed specifically for coastal chlorophyll concentrations. It is parameterized using a polynomial regression of the log-transformed ratio of R_{rs} at 490 and 555 nm and a weighted transform which blends to the global OC2v2 chlorophyll algorithm in offshore waters (Stumpf et al., 2000). Our satellite-derived values of $a_t(443)$, $a_{sd}(443)$, and $a_g(443)$ were compared to measurements from our seven recent field experiments in the northern Gulf of Mexico. Satellite matchups with sample locations were taken from either the same day or, if not available, a day either side of sampling. Our algorithms for satellite-derived a_{sd} and a_g were then applied to all satellite imagery for the time series analyses.

2.3. Physical forcing variables

We compiled time series of numerous physical forcing variables in the northern Gulf of Mexico (Table 1). These environmental variables were chosen as those that could plausibly affect tripton and CDOM concentrations in shelf surface waters. Daily measurements of water discharge for the Mississippi River were obtained from the United States Army Corps of

Engineers (USACE) for the Tarbert Landing, Louisiana station. Outflow from the Mississippi and Atchafalaya Rivers is highly in phase, reflecting efforts of the USACE to manage the discharge of the Mississippi River system so that ~2/3 of the discharge outflows via the bird-foot delta and the other 1/3 through the Atchafalaya (Fig. 1). Riverine outflow through Mobile Bay from the Alabama/Tombigbee Rivers (Fig. 1) is the next largest source of freshwater to the shelf. Daily measurements of riverine inputs to Mobile Bay were obtained from the United States Geological Survey (USGS) as a sum of discharges for the Alabama and Tombigbee Rivers. As well, river discharge with a 1-month lag for both the Mississippi and Alabama/Tombigbee Rivers was included in our analysis, to assess delayed response on the optical fields (e.g., buoyancy flux).

Other forcing variables used in our analyses were available as gridded fields from both satellites and data-assimilating models (Table 1). Wind speed and direction were obtained from the US Navy's Coupled Ocean/Atmosphere Mesoscale Prediction System (COAMPS) at ~30 km resolution. Photosynthetically available radiation (PAR) time series were constructed from SeaWiFS data, which compared well to PAR measured at the Louisiana Universities Marine Consortium (LUMCON) weather station ($r^2 = 0.94$). Accumulated rainfall was obtained from the Precipitation Radar as part of the Tropical Rainfall Measuring Mission (TRMM), with a horizontal resolution of ~1 km. Lastly, a data-assimilating physical circulation model was employed to obtain sea surface properties, including temperature (SST), salinity (SSS), height anomaly (SSH), current magnitude (SSM), and direction (SSU, SSV). We used the Northern Gulf of Mexico Ocean Nowcast/Forecast System (NGOMNFS) which consists of a 1/72° (1.9 km), 38-level sigma-*z* data-assimilating ocean model based on the Navy Coastal Ocean Model (NCOM) (Martin, 2000). The ocean model continuously assimilates satellite measurements of SSH from sensors such as Topex/Poseidon and SST from AVHRR and MODIS. Surface forcing to the ocean model is provided by surface wind stress, heat fluxes, solar radiation, air pressure, and river discharge, and the open boundary conditions are provided by the Intra-Americas Sea Ocean Nowcast/Forecast System (IASNFS; Ko et al., 2003; Chassignet et al., 2005). Results from the NGOMNFS model were available starting in 2002, which set the beginning year for our remote sensing study. We define both currents and winds in the *u* (zonal) and *v* (meridional) directions, where positive *u* is to the east and positive *v* is to the north. For our analysis, we interpolated all gridded forcing fields to the resolution of SeaWiFS imagery (~1 km). Mean monthly values were calculated for all forcing variables and SeaWiFS-derived products; thus, we cannot assess processes occurring at shorter time scales.

2.4. Time series analyses

Correlation and regression analyses were performed to analyze the impacts of the different forcing variables on driving mean monthly optical variability. For river discharge (and lagged discharge), Mississippi River flow was used throughout the southwest region of our study, which included most of the Louisiana shelf, and Alabama/Tombigbee flow was used in the northeast region of our study (latitude $>29.6°$ and longitude $>-90.7°$). In contrast, a unique physical time series at each image pixel was used for gridded forcing variables. Correlation analyses were performed between mean monthly satellite-derived time series of a_{sd} and a_g and each forcing variable for 2002–2004. As well, we used stepwise multiple linear regression analysis to determine the importance of the different variables in determining a_{sd} and a_g variability. A forward stepwise procedure was used in which the most statistically significant term (i.e., the lowest *p*-value for $p<0.05$) is added into the model at each step, until there are no statistically significant terms left to include. A common problem with multiple regression analysis is multicollinearity of the input variables, a point which we will discuss further, with reference to a cross-correlation matrix for all physical variables.

Multiple linear regression models were developed for both a_{sd} and a_g and each model's predictive capabilities were assessed. The a_{sd} and a_g models were developed at each image pixel using SeaWiFS and physical forcing time series from 2002 to 2004. Next, mean monthly environmental variables for 2005 were input to the models to determine how well temporal and spatial variability in a_{sd} and a_g could be predicted for a year that was not included in model development. The percent error in model predictions was assessed by comparing modeled imagery with SeaWiFS-derived imagery. In addition, representative scenarios were chosen to exemplify interannual and seasonal differences in a_{sd} and a_g

Table 1
Physical forcing variables for 2002– 2004 (mean monthly data)

Variable	Range	Units	Possible mechanism	a_{sd}[a]		a_g[a]	
				% Pixels[b]	Average r^2	% Pixels[b]	Average r^2
River discharge	Miss: 6.2×10^3–2.8×10^4 Al/Tom: 3.3×10^2–4.9×10^3	$m^3\,s^{-1}$	River input; advection; stratification	**17**	0.12	**16**	0.13
River discharge: 1-month lag	Miss: 6.2×10^3–2.8×10^4 Al/Tom: 3.3×10^2–4.9×10^3	$m^3\,s^{-1}$		*2*	0.09	**13**	**0.14**
Wind speed	3.3–7.5	$m\,s^{-1}$	Mixing	**36**	**0.21**	7	*0.06*
Wind *u* speed	−4.4 to 1.4	$m\,s^{-1}$	Advection	*3*	*0.04*	**34**	**0.14**
Wind *v* speed	−2.9 to 3.7	$m\,s^{-1}$	Advection	9	0.13	*3*	*0.06*
Solar radiation	20–54	$ein\,m^{-2}\,d^{-1}$	Stratification; Photo-oxidation (a_g)	Removed	**0.21**	Removed	0.07
Accumulated rainfall	0–873	mm	Dilution	6	*0.05*	*3*	*0.03*
Surface temperature (SST)	12–31	°C	Stratification	**12**	**0.17**	8	0.07
Surface salinity (SSS)	0–36		River input; advection	Removed	0.16	Removed	**0.15**
Surface height (SSH)	−0.40 to 3.0	m	Outwelling; stratification	Removed	0.12	Removed	**0.09**
Current speed (SSM)	0–1.5	$m\,s^{-1}$	Mixing	7	0.10	7	0.07
Current *u* speed (SSU)	−0.70 to 1.3	$m\,s^{-1}$	Advection	*4*	*0.08*	5	0.08
Current *v* speed (SSV)	−1.1 to 1.4	$m\,s^{-1}$	Advection	4	0.10	*4*	0.07

[a] In each column, the three highest values are in bold and the three lowest are italicized.
[b] As determined from stepwise regression analysis, the percent of pixels in which each variable was the most important predictor. Some variables were removed from the analysis based on high cross-correlations with other physical variables.

spatial distributions. For these scenarios, we showed how specific differences in the various physical forcing mechanisms were responsible for observed variability in SeaWiFS and modeled optical fields. All time series data analyses were performed using the MATLAB software package (The MathWorks).

3. Results

3.1. Spatial and temporal optical variability

We compared satellite-retrievals of bio-optical properties with absorption measurements from recent cruises in the northern Gulf of Mexico (Fig. 2). Of the 122 measured absorption spectra, we obtained 48 matchups with satellite imagery during cloud-free periods over the sampling sites. Measured values of absorption ranged from 9.7×10^{-2} to $6.4\,m^{-1}$ for $a_t(443)$, 6.7×10^{-3} to $3.6\,m^{-1}$ for $a_{sd}(443)$, and 4.6×10^{-2} to $1.4\,m^{-1}$ for $a_g(443)$. Significant relationships were observed between satellite-derived $a_t(443)$ and measured $a_t(443)$ (Fig. 2a, $r^2=0.82$, $p<0.001$), as well as satellite-derived $b_b(555)$ and measured $a_{sd}(443)$ (Fig. 2b, $r^2=0.83$, $p<0.001$), using power function fits. For total absorption, our comparison shows that $a_t(443)$ from the QAA model systematically underestimates measured values in this region. Thus, it is necessary to tune the QAA values with in situ data sets, as we have done here. For backscattering, although $b_b(555)$ has contributions from all suspended particles, we observed a less significant relationship between satellite-derived $b_b(555)$ and measured particulate absorption ($a_p(443)$; $r^2=0.75$) than with tripton alone ($a_{sd}(443)$; $r^2=0.83$). This result likely reflects the greater backscattering efficiency of inorganic particles and small (submicron) detrital particles compared to phytoplankton (e.g., Stramski and Kiefer, 1991; Green et al., 2003). We then used our corrected values of satellite-derived $a_t(443)$ and $a_{sd}(443)$ (Figs. 2A,B), as well as values for absorption by water and phytoplankton ($a_w(443)$ and $a_{ph}(443)$, see Section 2), to calculate CDOM absorption ($a_g(443)$) by difference. The resulting satellite-derived values for $a_g(443)$ were significantly related to measured values using a linear fit ($r^2=0.37$, $p<0.001$), with the slope not significantly different than one ($p<0.20$, Fig. 2c). Thus, no correction was applied to satellite-derived a_g values. The relationships between satellite-derived products and measured $a_t(443)$ and $a_{sd}(443)$ (Fig. 2) were used to calculate our final satellite-derived absorption values, which deviated from measured $a_t(443)$, $a_{sd}(443)$, and $a_g(443)$ by mean absolute errors of 32%, 51%, and 48%, respectively. These final satellite-derived products were used in the following time series analyses of $a_{sd}(443)$ and $a_g(443)$.

Significant spatial and temporal variability was observed in satellite-derived a_{sd} and a_g for mean monthly imagery from 2002 to 2004. We limited our analysis to relatively shallow shelf waters, generally within ~100 m depth, by setting lower limits for inclusion of $1.7\times10^{-2}\,m^{-1}$ for a_{sd} and 0.10 for a_g; all pixels below these values were removed from analysis (Fig. 3). In average imagery for the 2002–2004 time period, peak values of a_{sd} on the shelf were observed near the major river mouths (Atchafalaya, Mississippi, and Alabama/Tombigbee Rivers; Fig. 3A), corresponding to regions of high riverborne sediment delivery, whereas peak values of a_g were observed along much of the shoreline (Fig. 3B). CDOM absorption was generally higher than a_{sd} throughout our region of interest, except near the Mississippi and Atchafalaya River mouths where a_{sd} was higher. We also analyzed temporal variability in absorption time series, by choosing the maximum values from tripton and CDOM time series at each pixel. This analysis showed that a_{sd} peaked most often in the fall and winter in our region of interest (Fig. 3C), whereas a_g peaked most often in summer (Fig. 3D). However, a high degree of spatial variability was observed in peak timing depending on shelf location. These findings suggest significantly different physical forcing mechanisms for tripton and CDOM material on the shelf.

3.2. Correlation and stepwise regression analyses

To assess possible multi-collinearity, we constructed a cross-correlation matrix between physical forcing variables (Table 2). Significant correlations between variables were observed in several cases ($|r|>0.33$; two-tailed test, $\alpha=0.05$). The highest correlations were observed between wind speed and solar radiation ($r=-0.73$) and between SSH and SST ($r=0.83$; Table 2). Based on these results, both solar radiation and SSH were removed from the following multiple linear regression analyses. As well, we decided to remove SSS from the multiple linear regression analysis, because it was mostly redundant of the impacts of river discharge and lagged discharge on optical forcing; this decision will be further discussed.

Stepwise multiple linear regression analysis was used to determine which forcing variables were most important in driving optical variability during 2002–2004. The importance of each variable was calculated based on the number of pixels in which it was included in the stepwise model over our region of interest (for inclusion criteria, see Section 2). Based on this analysis, wind speed, river discharge, and SST were most often included in the model for a_{sd}, and wind u speed, river discharge, and lagged river discharge were most often included for a_g (Table 1). As the single most important variables, wind speed explained ~21% of the variability in a_{sd} (as an average over all pixels), and wind u speed explained ~14% of the variability in a_g (average r^2, Table 1).

For the most important physical driving variables, correlation maps were analyzed to assess temporal and spatial relationships

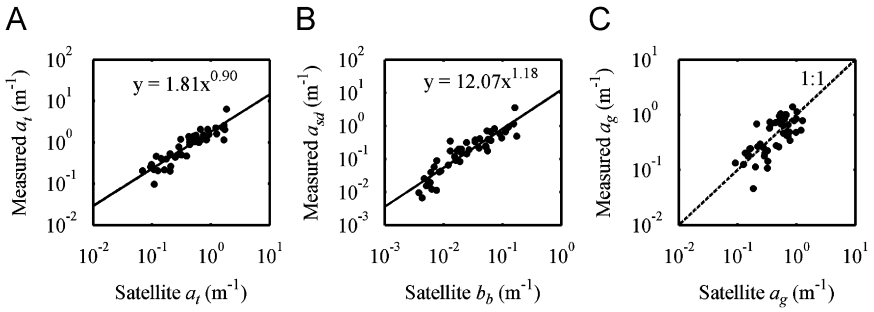

Fig. 2. Satellite algorithm development for total seawater absorption (a_t) and partitioned absorption by tripton and CDOM (a_{sd}, a_g). Power functions well fit relationships between (A) satellite-derived and measured $a_t(443)$, and (B) satellite-derived $b_b(555)$ and measured $a_{sd}(443)$. Satellite-derived a_g (panel C) were calculated by difference (see Section 2) and were related approximately 1:1 (dashed line) with measured a_g. Measured a_t, a_{sd}, and a_g values were collected during seven cruises in the northern Gulf of Mexico.

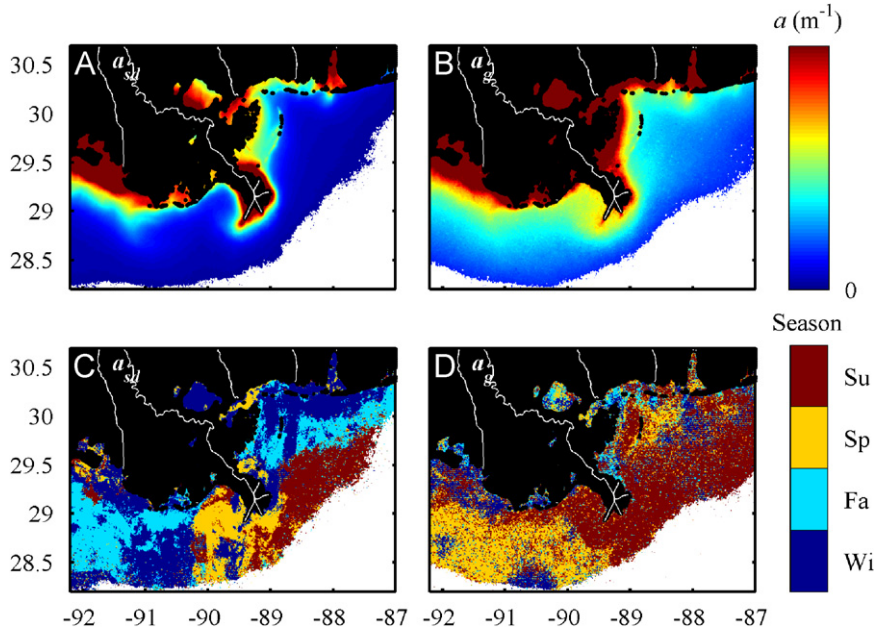

Fig. 3. For 2002–2004, average satellite-derived absorption by (A) tripton (a_{sd}) and (B) CDOM (a_g). Also, seasonal maxima in time series for both (C) a_{sd} and (D) a_g are shown. Seasons are defined as winter (December–February), spring (March–May), summer (June–August), and fall (September–November). Absorption values below our threshold of interest ($a_{sd} < 1.7 \times 10^{-2}\,m^{-1}$ and $a_g < 0.10\,m^{-1}$) were removed from analysis (white pixels).

Table 2
Correlation (r) matrix for physical forcing variables (2002–2004)

	DisM	DisA	DisLM	DisLA	WndS	WndU	WndV	PAR	Prec	SST	SSS	SSH	SSU	SSV	SSM
DisM	1.00														
DisA	**0.34**	1.00													
DisLM	**0.53**	0.02	1.00												
DisLA	**0.45**	**0.56**	0.31	1.00											
WndS	−0.07	**0.34**	**−0.42**	−0.01	1.00										
WndU	0.12	0.20	0.27	0.29	−0.29	1.00									
WndV	0.29	−0.07	**0.48**	0.13	**−0.51**	0.29	1.00								
PAR	0.24	**−0.38**	**0.58**	0	**−0.73**	0.10	**0.67**	1.00							
Prec	−0.15	0.05	−0.12	−0.06	−0.07	−0.13	0.28	0	1.00						
SST	−0.29	**−0.54**	0.06	**−0.41**	**−0.62**	0.01	**0.44**	**0.63**	**0.36**	1.00					
SSS	**−0.55**	−0.19	**−0.63**	**−0.40**	**0.50**	−0.23	**−0.49**	**−0.60**	0.02	−0.11	1.00				
SSH	−0.16	**−0.43**	0.02	−0.42	**−0.46**	**−0.35**	**0.43**	**0.57**	**0.38**	**0.83**	−0.17	1.00			
SSU	−0.01	0.10	0.18	0.18	−0.17	**0.54**	0.30	0.12	0.06	0.14	−0.10	−0.08	1.00		
SSV	0.12	−0.14	0.24	−0.02	−0.22	0.04	**0.47**	**0.35**	0.17	0.27	−0.21	0.28	0.25	1.00	
SSM	0.27	0.08	0.20	0.12	−0.05	−0.08	0.07	0.15	0.02	−0.04	**−0.41**	0.05	−0.10	0.04	1.00

$N = 36$. Absolute values greater than the critical value of 0.33 ($\alpha = 0.05$) are in bold. The correlations presented in this table for gridded fields are averages over the entire region of interest.
Variables: DisM = Mississippi River discharge, DisA = Alabama/Tombigbee River discharge, DisLM = 1-month lagged Mississippi River discharge, DisLA = 1-month lagged Alabama/Tombigbee River discharge, WndS = wind speed, WndU = wind u speed, WndV = wind v speed, Prec = precipitation.

with optical properties (Figs. 4 and 5). As expected, river discharge was usually the most important variable driving variability in a_{sd} and a_g near the river mouths (Fig. 4C, 5C). An exception was the low correlation observed between river discharge and a_g in Atchafalaya Bay. Positive relationships were observed between discharge and absorption (Fig. 4D, 5D), with peaks in discharge, a_{sd}, and a_g time series occurring in spring/summer near the Mississippi River mouth (e.g., Fig. 3C, D, 4D) and in winter/spring in the Alabama/Tombigbee outflow (e.g., Fig. 3C, D, 5D). SSS generally showed the same absolute correlation patterns with optical properties as did river discharge and lagged discharge (not shown), and high average correlations were observed between SSS and each of a_{sd} and a_g ($r^2 = 0.16$ and 0.15, respectively; Table 1). However, we chose not to include SSS in our final multiple linear regression analyses, because there were some important regions where river discharge (and lagged discharge) performed better in describing variability in optical properties, such as for a_{sd} near the Mississippi River delta. Away from river mouths, wind speed and SST were correlated with a_{sd} over large regions of the shelf (Fig. 4A, E). High correlations of a_{sd} with wind speed and SST generally occurred in regions where a_{sd} peaked in fall/winter. Wind speed was positively correlated with a_{sd} (Fig. 4B), whereas SST was negatively correlated with a_{sd} in nearshore waters (Fig. 4F). In the case of a_g, away from river mouths, all of wind u, discharge, and lagged discharge were important drivers of variability (Fig. 5). Wind u showed high, positive correlations with a_g to the east of the Mississippi River delta, in a region where both variables often peaked in summer (Fig. 5B).

Stepwise regression analyses were employed to better visualize the regions of influence of the most important variables driving changes in absorption. Three of these physical variables each for a_g and a_{sd} were solely included in separate stepwise

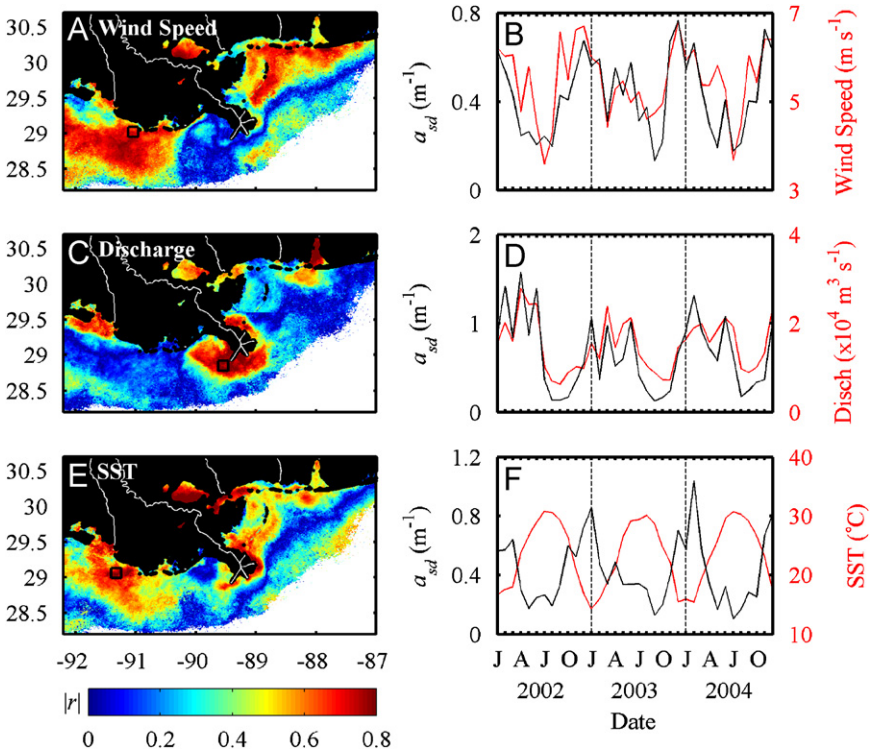

Fig. 4. For 2002–2004, absolute correlations (|*r*|) between sediment/detrital absorption (a_{sd}) and (A) wind speed, (C) river discharge, and (E) SST. At select locations of high correlation (square symbol in left-hand column), the time series for a_{sd} and each physical variable is plotted (right-hand column). Note that a_{sd} is positively correlated with wind speed and discharge, but negatively correlated with SST. The discontinuity in the discharge figure (panel C) at 29.6° latitude coincides with the boundary between a northern region where points were correlated with Alabama/Tombigbee discharge from Mobile Bay and a southern region where points were correlated with Mississippi River discharge.

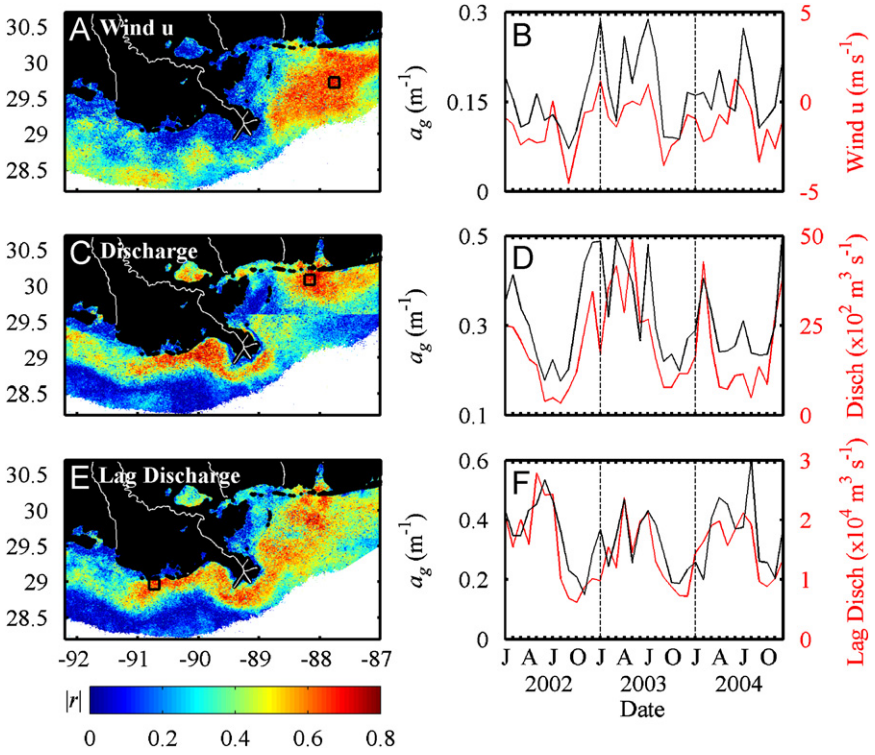

Fig. 5. For 2002–2004, absolute correlations (|*r*|) between CDOM absorption (a_g) and (A) wind *u* speed, (C) river discharge, and (E) lagged river discharge. At select locations of high correlation (square symbol in left-hand column), the time series for a_g and each physical variable is plotted (right-hand column). The discontinuity in the discharge figures (panels C and E) is described in the Fig. 4 caption.

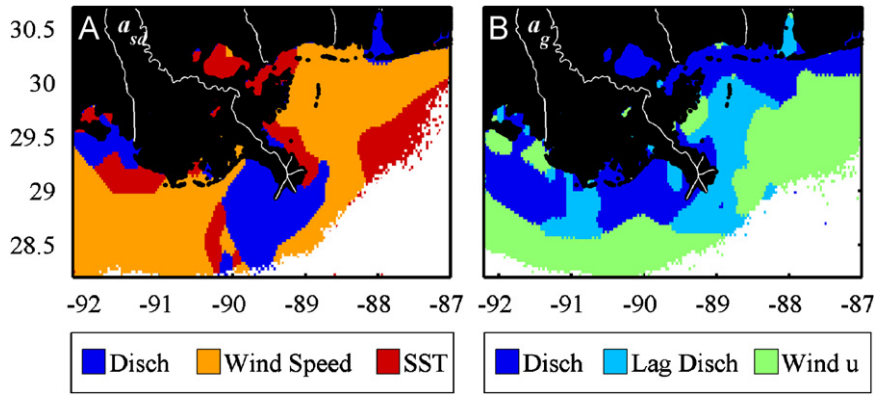

Fig. 6. For mean monthly time series (2002–2004), regions where each variable listed were the most important in driving a_{sd} and a_g. This was determined from stepwise multiple linear regression analysis for three of the most important variables for a_{sd} (wind speed, river discharge, and SST) and a_g (wind u speed, river discharge, and lagged discharge). Regions were smoothed to ease interpretation.

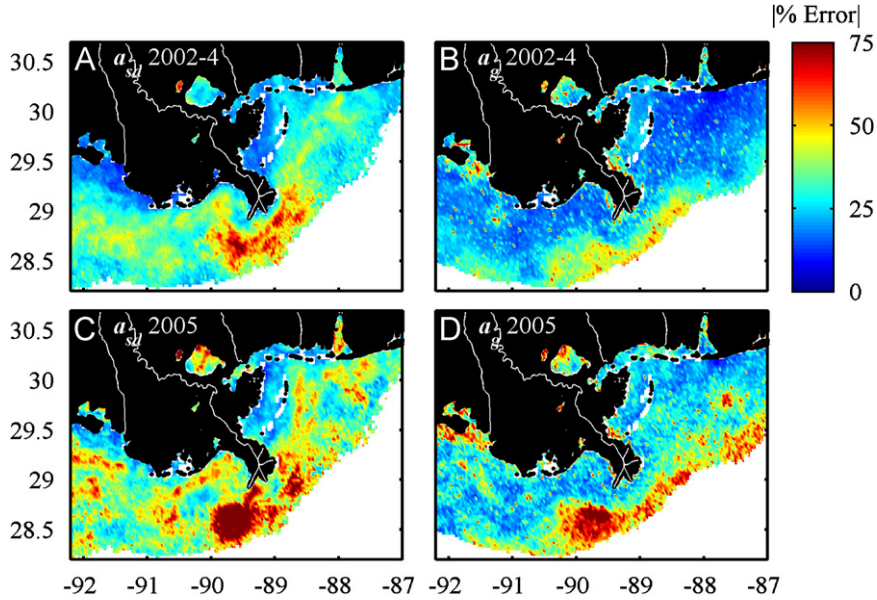

Fig. 7. Error analysis of average absolute differences between modeled and satellite-derived (A, C) a_{sd} and (B, D) a_g values. Multiple linear regression analysis was used to develop a_{sd} and a_g models at each pixel for model development years, 2002–2004 (upper panels). The model was then applied to environmental forcing variables for 2005 to determine how well the model could predict a_{sd} and a_g (lower panels).

analyses, and the single most important variable in determining variability at each pixel was chosen (minimum p-value) (Fig. 6). These figures re-emphasize the importance of discharge near the major river mouths, and the greater extent of this impact for CDOM in surface waters, compared to sediment/detritus. In the case of a_{sd}, wind speed and SST clearly dominate over regions of the shelf that are outside the direct influence of riverine inputs. For a_g, wind east–west speed (wind u) plays an important role in driving optical variability further offshore of the discharge-influenced regions.

3.3. *Performance of absorption models*

Multiple linear regression analysis was used to develop models for a_{sd} and a_g using SeaWiFS imagery and our data set of physical forcing variables (Table 1). As previously stated, several physical variables were not included in this analysis due to cross-correlation with other forcing variables, including solar radiation, SSH, and SSS. The remaining 10 physical variables (Table 1) were used at all pixels in both the a_{sd} and a_g multiple linear regression models, with each variable receiving its' own weighting in each pixel based on regression results. The models were developed using mean monthly imagery for 2002–2004. The predictive capabilities of the models were then tested by inputting physical time series for 2005 to the models and comparing the calculated a_{sd} and a_g values (magnitude and spatial pattern) with SeaWiFS-derived values. A comparison of satellite-derived and modeled optical properties resulted in average absolute errors of 32% and 29% for a_{sd} and a_g, respectively, in model development years (2002–2004) (Fig. 7A,B). As expected, errors were higher in 2005, averaging 41% and 46% for a_{sd} and a_g, respectively (Fig. 7C, D).

The generally good comparison between modeled and satellite-derived values allowed us to describe the physical forcing mechanisms responsible for temporal and spatial differences in tripton and CDOM distributions. We present an example each of interannual and seasonal variability, incorporating examples from 2005, to further demonstrate the model's predictive capabilities. Significantly different tripton distributions were observed in April 2002 compared to April 2005, and these differences were well

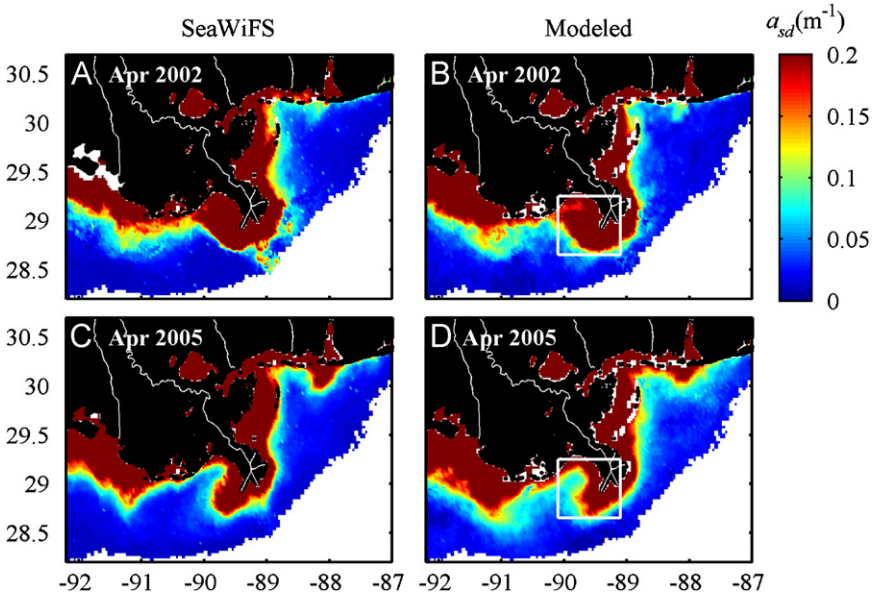

Fig. 8. Interannual variability in SeaWiFS (left column) and multiple linear regression model-derived (right column) a_{sd} distributions, comparing April of 2002 and 2005. The model was developed using mean monthly imagery for 2002–2004, such that the 2005 example represents the predictive capabilities of the model. An example of differences between years is discussed in Section 3 (white boxes; right column).

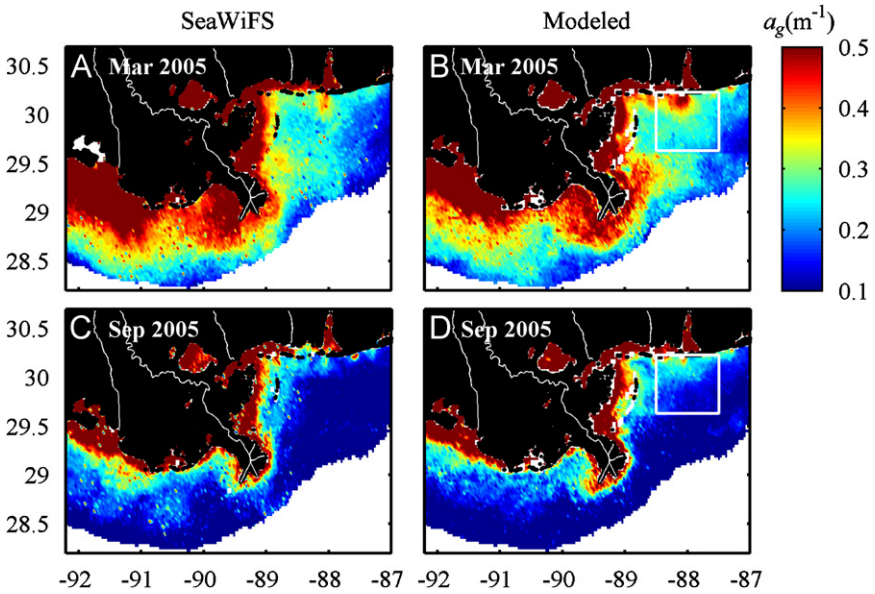

Fig. 9. Seasonal variability in SeaWiFS (left column) and multiple linear regression model-derived (right column) a_g distributions, comparing March and September 2005. An example of seasonal differences is discussed in Section 3 (white boxes; right column).

represented in model results (Fig. 8). For example, the Mobile Bay plume extended further onto the shelf in April 2005. Also, lower tripton concentrations were observed in the Louisiana Bight in 2005 (see white box, Fig. 8B, C). To better understand the mechanisms causing this difference, we compared physical forcing factors between April 2002 and 2005 and used our model to determine which factors were most responsible for the interannual variability in the observed a_{sd} values in the Louisiana Bight. Differences in Mississippi River discharge were primarily responsible for variable a_{sd}, with discharge 1.5 × higher in April 2002. The second most important driving variable was east–west wind speed (WndU), with the expected effects of higher wind speed to the west in April 2002 causing the plume to extend further into the Louisiana Bight. The third most important variable was wind speed (WndS) which was higher in April 2005 (6.1 m s^{-1} versus 4.8 m s^{-1} in April 2002), and which potentially counteracted the effects of the Coriolis force and/or caused higher vertical mixing losses of tripton from surface waters.

Seasonal variability was also well represented in model predicted optical properties. For example, significantly different CDOM distributions on the shelf were observed between March and September 2005 in both satellite-derived and modeled imagery (Fig. 9). In general, higher a_g values were observed throughout the study region in March, including in the Atchafalaya, Mississippi, and Alabama/Tombigbee River plumes. We compared differences in physical forcing variables between March and September and used our model to determine which factors were most responsible for observed differences in a_g south of

Mobile Bay (see white box, Fig. 9B,D). Differences in wind u speed were primarily responsible for differences in a_g, with the expected effects of winds directed to the east in March and to the west in September. The second most important driving variable was Alabama/Tombigbee River discharge, which was much higher in March ($2.7 \times 10^3\,m^3\,s^{-1}$) compared to September ($0.9 \times 10^3\,m^3\,s^{-1}$). Finally, the third most important variable was Alabama/Tombigbee River discharge lagged by 1 month, which was also higher in March and contributed to higher a_g on the shelf. These examples demonstrate that the models are able to capture the observed spatial and temporal variability in the optical fields, and that they can help elucidate the physical forcing mechanisms controlling a_{sd} and a_g distributions in these highly dynamic shelf waters.

4. Discussion

4.1. Spatial and temporal optical variability

In northern Gulf of Mexico shelf waters, absorption by tripton and CDOM was generally highest nearshore, and CDOM dominated total absorption as a spatial average over our region-of-interest ($\bar{a}_{sd} = 0.26, \bar{a}_g = 0.41$). Previous observations based on cruise measurements also showed particulate and CDOM absorptions decreasing with increasing salinity in shelf waters (D'Sa and Miller, 2003). Absorption by CDOM was the major component of total absorption, as seen in average imagery (Fig. 3B), usually exceeding contributions from tripton (Fig. 3A) and phytoplankton (Green and Gould, 2008). The main exceptions were near the major riverine outputs from the Mississippi and Atchafalaya, where particulates were often the dominant component (Fig. 3A, B). Previously published values for a cruise in the Louisiana Bight in March 2002 showed that a_g contributed on average from 37% to 64% to total absorption, in a region highly impacted by riverine waters (D'Sa et al., 2006). Away from river-dominated waters, our cruise measurements showed a_g contributions as high as 80–90% of total absorption in shelf waters. Whereas peak tripton absorption was mainly observed near river mouths (Fig. 3A), peaks in CDOM absorption occurred along most of the coast (Fig. 3B), including shallow waters that interact with coastal wetlands. Wetlands along the Louisiana coast can be active sources of DOC injection (references in Guo et al., 1999; Engelhaupt and Bianchi, 2001), as observed in CDOM fluorescence measurements on the shelf (Hitchcock et al., 2004). Following biological uptake, DOC from Louisiana coastal wetlands may be an important contributor to the formation of summertime hypoxia in shelf coastal waters (e.g., Green et al., 2006).

Seasonality in peak absorption differed between tripton and CDOM and depended upon shelf location. Near the Mississippi River delta, tripton absorption peaked in spring and CDOM absorption peaked slightly later, in summer (Fig. 3C,D). This finding corresponds well with measurements of peak SPM and particulate organic carbon (POC) concentrations in the Mississippi River in springtime (Bianchi et al., 2007), versus later peaks observed in riverine DOC in summer (Duan et al., 2007), for the period of our study. Over the entire shelf, absorption by CDOM generally peaked in either spring or summer (Fig. 3D). Patterns in CDOM peak timing were similar to those previously observed for phytoplankton absorption (Green and Gould, 2008), suggesting similar forcing mechanisms for the two optical groups. For example, both DOC and nitrate in the Mississippi River peaked in summer during 2002–2004, which would positively affect CDOM and phytoplankton, respectively, on the shelf. In contrast, in open waters of the Gulf of Mexico, satellite estimates of combined tripton and CDOM absorption (most of which we assume is CDOM) showed peak values in the winter (Jolliff et al., 2008). In shelf waters, we observed significantly different peak timing for tripton compared to CDOM, with tripton peaks often occurring in fall and winter on the shelf (Fig. 3C). Differences in peak timing for non-living optical groups (particulate versus dissolved) indicate substantially different forcing mechanisms in shelf waters.

4.2. Environmental forcing of tripton and CDOM

Relationships with river discharge illustrate the importance of particle sinking close to river mouths versus the longer distance advection of CDOM on the shelf. River discharge appears to be an important driver of all three absorption components in shelf waters, including tripton (Fig. 4E), CDOM (Fig. 5C), and phytoplankton (Green and Gould, 2008). High correlations between river discharge and tripton absorption are observed only near the river mouths (Fig. 4C). This suggests rapid particle sinking from the river plume, as indicated by high sediment accumulation rates near the Mississippi River mouth (Corbett et al., 2006). For the Mississippi River plume, previous satellite-based observations have demonstrated strong positive correlations between river discharge and suspended sediment loads in the plume (e.g., Walker, 1996). In particular, the pattern of high spatial correlation we observed between discharge and tripton in the Mississippi River plume during 2002–2004 was similar to that observed in SeaWiFS imagery for 1997–2000 (Salisbury et al., 2004). In contrast to tripton, high positive correlations were observed between discharge and CDOM (Fig. 5C) at greater distances from river mouths, indicative of greater horizontal advection of riverine CDOM. The one exception was the Atchafalaya River outflow for which no correlation was observed between river discharge and CDOM, presumably due to local production and exchange within coastal wetlands along the lower Atchafalaya which are absent along the lower Mississippi (Chen and Gardner, 2004). These processes in the lower Atchafalaya River may mask any correlation between discharge and CDOM in that region. For the Mississippi River, the long distance advection of riverine CDOM has previously been observed extending all the way to the West Florida Shelf (e.g., Del Castillo et al., 2001).

Although discharge was an important determinant of optical properties, winds were the single most important predictor of tripton and CDOM absorption across the shelf region of our study. Wind speed was the best predictor of a_{sd} (Fig. 4A), whereas wind u (east–west) speed was the best predictor of a_g (Fig. 5A). The spatial correlation pattern which we observed between wind speed and tripton was similar to that previously reported using SeaWiFS data for 1997–2000 (Salisbury et al., 2004). However, compared to the previous study, we did observe higher wind–detritus correlations in shallow nearshore waters (e.g., Terrebonne Bay and near the Chandaleur Islands, Fig. 4A), possibly due to differences in satellite-based algorithms between studies. The importance of wintertime cold-fronts in driving sediment resuspension in these shallow regions of the northern Gulf of Mexico has been demonstrated (Perez et al., 2000; Walker and Hammack, 2000). High wind–detritus correlations at deeper depths of 20–50 m are probably explained by resuspension in shallow waters followed by offshore transport occurring in the presence of wintertime north winds (Allison et al., 2000; Salisbury et al., 2004). It appears that wind and related wave forcing significantly change surface tripton distributions and increase the total horizontal flux over the shelf, as has been reported in other river-dominated shelf regions, such as the northern Adriatic Sea (Wang et al., 2007). Although resuspension of CDOM from benthic sources has been observed in other shelf

regions (Boss et al., 2001), we suggest that this is not an important process in northern Gulf of Mexico waters, given the low correlations we observed between wind speed and CDOM absorption (not shown). However, wind east–west speed did play an important role in the horizontal advection of CDOM on the shelf (Fig. 5A), especially east of the Mississippi River delta. As expected, winds and corresponding currents (SSU, Table 2) to the east, often in summer (Fig. 5A; Salisbury et al., 2004), were responsible for higher concentrations of CDOM to the east of the Mississippi and Alabama/Tombigbee River outlets.

Additionally, thermal stratification appears to play an important role in controlling tripton absorption in northern Gulf of Mexico shelf waters, based on relationships with SST. We emphasize that the regression methods we present in this paper are statistical models which can only represent relationships between variables and, for this reason, are more limited than mechanistic models. Thus, we can only speculate as to the underlying causal mechanisms by which a physical variable might drive optical variability. We observed high, negative correlations between a_{sd} and SST in nearshore waters (Fig. 4E,F), where a_{sd} often peaked in winter when SST was lowest. This suggests that thermal stratification and its' effects on mixing may play an important role in determining a_{sd} distributions. In winter, the combination of low solar heating and cold river inflow which moves out over warmer underlying Gulf water creates a vertical instability in the water column. We speculate that this thermal instability potentially decreases the wind speed threshold required to mix detritus up into surface waters, thus facilitating resuspension processes during the winter.

In addition to physical processes, biological processes will also have significant effects on tripton and CDOM distributions on the shelf. Although the focus of our modeling study was on understanding physical processes which affect distributions of non-living optical properties, we briefly examined the spatial correlations between surface phytoplankton, tripton, and CDOM distributions (Fig. 10). The tripton absorption coefficient, a_{sd}, represents absorption by both inorganic sediments and organic detritus. In shallow coastal waters and near riverine sources, the highest contributions of inorganic sediments to a_{sd} will be observed. In deeper offshore regions, absorption by organic detritus will become more important, resulting in the higher observed correlations between a_{sd} and phytoplankton absorption offshore (Fig. 10A). CDOM absorption shows significant and positive relationships with phytoplankton absorption over a larger region of the shelf (Fig. 10B). However, it is difficult to determine from our analysis whether CDOM distributions were influenced by biological production, or whether similar physical mechanisms control both their distributions. For example, river discharge positively affects both CDOM (Fig. 5C) and phytoplankton (Green and Gould, 2008) over a large region of the shelf, and both CDOM and phytoplankton concentrations appear to have similar seasonality on the shelf (Gould et al., 2007), as well as in the open Gulf (Jolliff et al., 2008). Cruise measurements and modeling results have shown significant contributions of biological processes to both detritus (e.g., Green et al., 2008) and dissolved organic carbon (e.g., Benner and Opsahl, 2001) in the Mississippi River plume. Furthermore, biological contributions to CDOM have been observed at depth, corresponding to sub-surface chlorophyll maxima, and mixed into surface waters during periods of higher winds, such as in spring (Chen et al., 2004). Although biological impacts on non-living optical properties are probably important on the shelf, with our statistical approach, it is difficult to separate potential biological forcing from physical forcing which may similarly affect living and non-living optical components in some regions.

4.3. Predictive optical models

An ultimate goal of research in optical oceanography is the development of predictive models for forecasting oceanic property distributions, especially in highly complex coastal regions. Predictive optical models are important to a broad range of applications, including forecasting light availability for phytoplankton growth (e.g., harmful algal bloom species), adaptive cruise sampling of transient events (e.g., river plumes), and underwater visibility for naval and maritime operations (e.g., Dickey et al., 2006). For northern Gulf of Mexico shelf waters, our statistical models for tripton and CDOM absorption performed well in predicting surface distributions in 2005, with average errors of 41% and 46% for a_{sd} and a_g, respectively (Fig. 7C,D). We feel that these results were particularly good given the range of unique optical sources in our region of interest, including inputs from large rivers, coastal wetlands and bays, and resuspension from shallow bottom waters. Given the importance of optical prediction, forays are now being made into the development of numerical models for predicting optical properties in coastal waters. As a first step, the optical properties can be treated as simple passive tracers in a circulation model, to assess the extent that dynamics control the optical distributions (Gould et al., 2007). The next step is to add complexity through development of coupled optical/ecological models. Such a model was developed for the West Florida Shelf, and showed that the Gulf of Mexico Loop Current significantly affected optical properties in summer, while high freshwater inputs were mainly responsible for optical variability in fall (Bissett et al., 2005). We anticipate that results from our research will provide insights and guidance for future development of similar optical/ecological models for the northern Gulf of Mexico (e.g., Green et al., 2008). We observed that variability in non-living optical properties on the shelf was

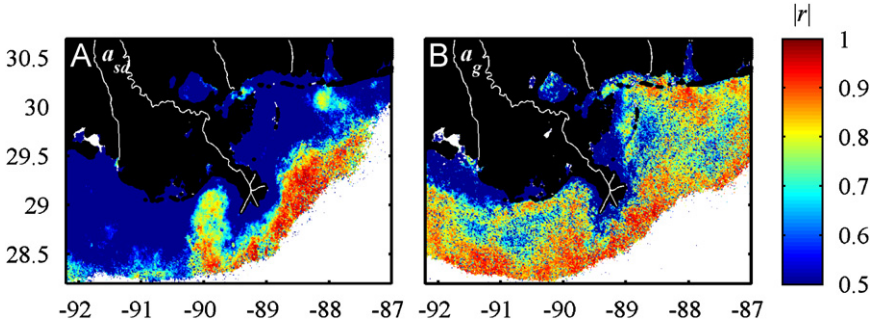

Fig. 10. For 2002–2004, absolute correlations (|r|) between phytoplankton absorption (a_{ph}) and each of (A) tripton absorption (a_{sd}) and (B) CDOM absorption (a_g). Correlation coefficients were positive in all regions of high correlation. Note, we used a different colorscale axis than in Figs. 4 and 5 to accommodate high correlations observed with a_{ph} in some regions.

significantly related to river discharge, wind speed, and wind direction, as well as to SST, which was likely an indicator of thermal stratification.

There is growing interest in the use of physical circulation models to describe optical variability in the coastal ocean. Recent advances in circulation modeling for coastal regions have made this goal more attainable (e.g., Hetland and DiMarco, 2007; Ko et al., 2007). Several field studies have demonstrated the effects of currents on optically active constituents in the water column, including measurements from the Coastal Mixing and Optics experiment on the New England Shelf (e.g., Chang and Dickey, 2001) and the Hyperspectral Coastal Ocean Dynamics Experiment in New York Bight waters (e.g., Chang et al., 2002). As well, in the northern Gulf of Mexico, analysis of measured currents indicated that 70% of backscattering variability was due to onshore currents during summer months at the shelf edge Gallegos et al., 2005). One of our interests in the present study was to determine how well modeled physical fields from the NGOMNFS model could predict optical properties in our region of study. Modeled sea surface salinity (SSS) often showed similar correlation patterns as river discharge to optical properties, explaining on average 15–16% of variability in a_{sd} and a_g (Table 1). Modeled current parameters (speed and direction) individually described only 7–10% (on average) of variability in a_{sd} and a_g (Table 1), though in specific regions the amount of variability described was much higher (50–60%; not shown). Given known challenges in accurately modeling buoyancy flux in coastal waters, further validation of circulation model results with current and density measurements will certainly lead to improvements in these models in river-dominated regions. It will be interesting to see whether future circulation models for northern Gulf shelf waters describe more of the observed optical variability.

5. Conclusions

The ocean color algorithms presented here provide a new capability for understanding variability in the distinct optical constituents of shelf surface waters in the northern Gulf of Mexico. The development of our empirical algorithms relied heavily on coastal cruise measurements collected in different seasons throughout several years in the region. In comparison to our previous work with phytoplankton (Green and Gould, 2008), we show that CDOM is the primary contributor to total absorption over much of the shelf region of our study. We observed distinct seasonal timing in tripton and CDOM absorption on the shelf, with wintertime resuspension events notably affecting tripton distributions and summertime peaks in river discharge and eastward winds driving advection of CDOM. In addition to discharge and winds, the correlation of SST with a_{sd} strongly suggests the additional impacts of thermal stratification on vertical mixing and resuspension of particles. Previously, relationships have been observed between surface water constituents and salinity on the shelf (e.g., Trefry et al., 1992; Benner and Opsahl, 2001). Similarly, we observed high correlations between optical properties and SSS derived from a hydrodynamic model, although not always as robust as correlations between optical properties and river discharge. In the future, a more accurate model-derived salinity product would likely help to improve models for detritus and CDOM, as well as elucidating biological contributions to non-living optical properties through the use of two end-member mixing models. For this region, important avenues of future research will also include time series analyses at higher temporal resolution, on the order of several days to weekly timescales, and at higher spatial resolution to better study the importance of organic matter inputs from shallow, coastal bays and estuaries.

Acknowledgements

This work was supported by an NRC Research Associateship award to R. Green, and NRL Program PE0601153N and NASA grant NNH04AB02I to R. Gould. We thank S. Lohrenz and R. Greene for the opportunity to participate on recent cruises, W. Goode for assistance in cruise preparation, and P. Martinolich for programming and image processing. This manuscript was significantly improved through the thoughtful comments of M. Pinkerton and two anonymous reviewers.

Appendix A. Supplementary data

Supplementary data associated with this article can be found in the online version at doi:10.1016/j.csr.2008.02.019

References

Allison, M.A., Kineke, G.C., Gordon, E.S., Goni, M.A., 2000. Development and reworking of a seasonal flood deposit on the inner continental shelf off the Atchafalaya River. Continental Shelf Research 20 (16), 2267–2294.

Arnone, R.A., Martinolich, P., Gould Jr., R.W., Sydor, M., Stumpf, R., Ladner, S., 1998. Coastal optical properties using SeaWiFS. In: Ocean Optics XIV Meeting, Kona, HA.

Benner, R., Opsahl, S., 2001. Molecular indicators of the sources and transformations of dissolved organic matter in the Mississippi river plume. Organic Geochemistry 32 (4), 597–611.

Bianchi, T.S., Filley, T., Dria, K., Hatcher, P., 2004. Temporal variability in sources of dissolved organic carbon in the lower Mississippi River. Geochimica et Cosmochimica Acta 68, 959–967.

Bianchi, T.S., Wysocki, L.A., Stewart, M., Filley, T.R., McKee, B.A., 2007. Temporal variability in terrestrially-derived sources of particulate organic carbon in the lower Mississippi River and its upper tributaries. Geochimica et Cosmochimica Acta 71, 4425–4437.

Bissett, W.P., Arnone, R., DeBra, S., Dieterle, D.A., Dye, D., Kirkpatrick, G.J., Schofield, O.M., Vargo, G.A., 2005. Predicting the optical properties of the West Florida Shelf: resolving the potential impacts of a terrestrial boundary condition on the distribution of colored dissolved and particulate matter. Marine Chemistry 95 (3–4), 199–233.

Boss, E., Pegau, W.S., Zaneveld, J.R.V., Barnard, A.H., 2001. Spatial and temporal variability of absorption by dissolved material at a continental shelf. Journal of Geophysical Research 106 (C5), 9499–9507.

Chang, G.C., Dickey, T.D., 2001. Optical and physical variability on timescales from minutes to the seasonal cycle on the New England shelf: July 1996 to June 1997. Journal of Geophysical Research 106 (C5), 9435–9453.

Chang, G.C., Dickey, T.D., Schofield, O.M., Weidemann, A.D., Boss, E., Pegau, W.S., Moline, M.A., Glenn, S.M., 2002. Nearshore physical processes and bio-optical properties in the New York Bight. Journal of Geophysical Research 107 (C9) (Art. no. 3133).

Chassignet, E.P., Hurlburt, H.E., Smedstad, O.M., Barron, C.N., Ko, D.S., Rhodes, R.C., Shriver, J.F., Wallcraft, A.J., Arnone, R.A., 2005. Assessment of data assimilative ocean models in the Gulf of Mexico using ocean color. In: Sturgers, W., Lugo-Fernandes, A. (Eds.), Circulation in the Gulf of Mexico: Observations and Models, AGU Monograph Series, vol. 161, Washington, DC, pp. 87–100.

Chen, R.F., Gardner, G.B., 2004. High-resolution measurements of chromophoric dissolved organic matter in the Mississippi and Atchafalaya River plume regions. Marine Chemistry 89 (1–4), 103–125.

Chen, R.F., Bissett, P., Coble, P., Conmy, R., Gardner, G.B., Moran, M.A., Wang, X.C., Wells, M.L., Whelan, P., Zepp, R.G., 2004. Chromophoric dissolved organic matter (CDOM) source characterization in the Louisiana Bight. Marine Chemistry 89 (1–4), 257–272.

Corbett, D.R., Mckee, B., Allison, M., 2006. Nature of decadal-scale sediment accumulation on the western shelf of the Mississippi River delta. Continental Shelf Research 26 (17–18), 2125–2140.

Dagg, M.J., Whitledge, T.E., 1991. Concentrations of copepod nauplii associated with the nutrient-rich plume of the Mississippi River. Continental Shelf Research 17, 845–857.

Dagg, M., Benner, R., Lohrenz, S., Lawrence, D., 2004. Transformation of dissolved and particulate materials on continental shelves influenced by large rivers: plume processes. Continental Shelf Research 24 (7–8), 833–858.

Del Castillo, C.E., Coble, P.G., Conmy, R.N., Muller-Karger, F.E., Vanderbloemen, L., Vargo, G.A., 2001. Multispectral in situ measurements of organic matter and chlorophyll fluorescence in seawater: documenting the intrusion of the Mississippi River plume in the West Florida Shelf. Limnology and Oceanography 46 (7), 1836–1843.

Dickey, T., Lewis, M., Chang, G., 2006. Optical oceanography: recent advances and future directions using global remote sensing and in situ observations. Reviews of Geophysics 44 (1) (Art. no. RG1001).

Duan, S.W., Bianchi, T.S., Sampere, T.P., 2007. Temporal variability in the composition and abundance of terrestrially-derived dissolved organic matter in the lower Mississippi and Pearl Rivers. Marine Chemistry 103 (1–2), 172–184.

D'Sa, E.J., Miller, R.L., 2003. Bio-optical properties in waters influenced by the Mississippi River during low flow conditions. Remote Sensing of the Environment 84 (4), 538–549.

D'Sa, E.J., Miller, R.L., Del Castillo, C., 2006. Bio-optical properties and ocean color algorithms for coastal waters influenced by the Mississippi River during a cold front. Applied Optics 45 (28), 7410–7428.

D'Sa, E.J., Miller, R.L., Mckee, B.A., 2007. Suspended particulate matter dynamics in coastal waters from ocean color: application to the northern Gulf of Mexico. Geophysical Research Letters 34 (Art. no. L23611).

Engelhaupt, E., Bianchi, T.S., 2001. Sources and composition of high-molecular-weight dissolved organic carbon in a southern Louisiana tidal stream (Bayou Trepagnier). Limnology and Oceanography 46 (4), 917–926.

Gallegos, S.C., Gould, R.W., Arnone, R.A., Teague, W.J., Mitchell, D.A., Ko, D.S., 2005. Analysis of the spectral backscattering coefficient variability on the northeastern shelf of the Gulf of Mexico. In: Eos Trans. AGU Meeting, New Orleans, LA.

Gould Jr., R.W., Green, R.E., Martinolich, P.M., Smith, R., Townsend, T.L., 2007. Multi-year optical variability in the Northern Gulf of Mexico: impact of atmospheric and oceanic forcing. In: AGU Joint Assembly Meeting, Acapulco, Mexico.

Green, R.E., Gould Jr., R.W., 2008. A predictive model for satellite-derived phytoplankton absorption over the Louisiana shelf hypoxic zone: effects of nutrients and physical forcing, Journal of Geophysical Research, doi:10.1029/2007JC004594, in press.

Green, R.E., Sosik, H.M., Olson, R.J., 2003. Contributions of phytoplankton and other particles to inherent optical properties in New England continental shelf waters. Limnology and Oceanography 48, 2377–2391.

Green, R.E., Bianchi, T.S., Dagg, M.J., Walker, N.D., Breed, G.A., 2006. An organic carbon budget for the Mississippi River turbidity plume and plume contributions to air–sea CO_2 fluxes and bottom water hypoxia. Estuaries and Coasts 29, 579–597.

Green, R.E., Breed, G.A., Dagg, M.J., Lohrenz, S.E., 2008. Modeling the response of primary production and sedimentation to variable nitrate loading in the Mississippi River plume. Continental Shelf Research, in press, doi:10.1016/j.csr.2007.02.008.

Guo, L., Santschi, P.H., Bianchi, T.S., 1999. Dissolved organic matter in estuaries of the Gulf of Mexico. In: Bianchi, T.S., Pennock, J.R., Twilley, R.R. (Eds.), Biogeochemistry of Gulf of Mexico Estuaries. Wiley, New York, pp. 269–299.

Hetland, R.D., DiMarco, S.F., 2007. How does the character of oxygen demand control the structure of hypoxia on the Texas–Louisiana continental shelf? Journal of Marine Systems doi:10.1016/j.jmarsys.2007.03.002.

Hitchcock, G.L., Chen, R.F., Gardner, G.B., Wiseman, W.J., 2004. A Lagrangian view of fluorescent chromophoric dissolved organic matter distributions in the Mississippi River plume. Marine Chemistry 89 (1–4), 225–239.

Jolliff, J.K., Kindle, J.C., Penta, B., Helber, R., Lee, Z., Shulman, I., Arnone, R., Rowley, C.D., 2008. On the relationship between satellite-estimated bio-optical and thermal properties in the Gulf of Mexico. Journal of Geophysical Research, Biogeosciences, in press, doi:10.1029/2006JG000373.

Kishino, M., Takahashi, N., Okami, N., Ichimura, S., 1985. Estimation of the spectral absorption coefficients of phytoplankton in the sea. Bulletin of Marine Science 37, 634–642.

Ko, D.S., Preller, R.H., Martin, P.J., 2003. An experimental real-time intra Americas sea ocean nowcast/forecast system for coastal prediction. In: AMS Fifth Conference on Coastal Atmospheric & Oceanic Prediction & Processes, Seattle, WA, pp. 97–100.

Ko, D.S., Martin, P.J., Rowley, C.D., Preller, R.H., 2007. A real-time coastal ocean prediction experiment for MREA04. Journal of Marine Systems doi:10.1016/j.jmarsys.2007.02.022.

Lee, Z.P., Carder, K.L., Arnone, R.A., 2002. Deriving inherent optical properties from water color: a multiband quasi-analytical algorithm for optically deep waters. Applied Optics 41 (27), 5755–5772.

Lee, Z.P., Weidemann, A., Kindle, J., Arnone, R., Carder, K.L., Davis, C., 2007. Euphotic zone depth: its derivation and implication to ocean-color remote sensing. Journal of Geophysical Research 112 (C3), 0 (Art. no. C03009).

Lohrenz, S.E., Fahnenstiel, G.L., Redalje, D.G., Lang, G.A., Dagg, M.J., Whitledge, T.E., Dortch, Q., 1999. Nutrients, irradiance, and mixing as factors regulating primary production in coastal waters impacted by the Mississippi River plume. Continental Shelf Research 19, 1113–1141.

Maritorena, S., Siegel, D.A., Peterson, A.R., 2002. Optimization of a semianalytical ocean color model for global-scale applications. Applied Optics 41 (15), 2705–2714.

Martin, P.J., 2000. Description of the Navy Coastal Ocean Model Version 1.0. Technical Report NRL/FR/7322-00-9962, 42pp.

Martinolich, P.M., 2005. In: Naval Research Laboratory (Ed.), Automated Processing System User's Guide Version 3.4 See 〈http://www7333.nrlssc.navy.mil/docs/aps_v3.4/user/aps/〉.

Meade, R.H., 1996. River-sediment inputs to major deltas. In: Milliman, J., Haq, B.U. (Eds.), Sea-level Rise and Coastal Subsidence. Kluwer Academic Publishers, Dordrecht, Netherlands, pp. 63–85.

Perez, B.C., Day, J.W., Rouse, L.J., Shaw, R.F., Wang, R., 2000. Influence of Atchafalaya River discharge and winter frontal passage on suspended sediment concentration and flux in Fourleague Bay, Louisiana. Estuarine, Coastal and Shelf Science 50 (2), 271–290.

Pope, R.M., Fry, E.S., 1997. Absorption spectrum (380–700 nm) of pure water. II. Integrating cavity measurements. Applied Optics 36, 8710–8723.

Rabalais, N.N., Turner, R.E., Wiseman Jr., W.J., 2002. Gulf of Mexico hypoxia, a.k.a. "The Dead Zone". Annual Review of Ecology and Systematics 33, 235–263.

Ransibrahmanakul, V., Stumpf, R.P., 2006. Correcting ocean colour reflectance for absorbing aerosols. International Journal of Remote Sensing 27, 1759–1774.

Salisbury, J.E., Campbell, J.W., Lindner, E., Meeker, L.D., Muller-Karger, F.E., Vorosmarty, C.J., 2004. On the seasonal correlation of surface particle fields with wind stress and Mississippi discharge in the northern Gulf of Mexico. Deep-Sea Research II 51, 1187–1203.

Stramski, D., Kiefer, D.A., 1991. Light-scattering by microorganisms in the open ocean. Progress in Oceanography 28, 343–383.

Stumpf, R.P., Arnone, R.A., Gould, R.W., Martinolich, P., Ransibrahmanakul, V., Tester, P.A., Steward, R.G., Subramaniam, A., Culver, M., Pennock, J.R., 2000. SeaWiFS ocean color data for US Southeast coastal waters. In: Sixth International Conference on Remote Sensing for Marine and Coastal Environments, Ann Arbor, MI, pp. 25–27.

Stumpf, R.P., Arnone, R.A., Gould Jr., R.W., Martinolich, P.M., Ransibrahmanakul, V., 2003. A partially-coupled ocean–atmosphere model for retrieval of water-leaving radiance from SeaWiFS in coastal waters. In: Hooker, S.B., et al. (Eds.), Algorithm Updates for the Fourth SeaWiFS Data Reprocessing, vol. 22, NASA Technical Memo 2002–206892. NASA Goddard Space Flight Center, Greenbelt, MD.

Trefry, J.H., Trocine, R.P., Metz, S., Nelsen, T.A., Hawley, N., 1992. Suspended particulate matter on the Louisiana shelf: concentrations, composition and transport pathways. In: Proceedings of the NECOP Workshop, October 1991. Sea-Grant Publications, Cocodrie, LA, pp. 126–130.

Van der Leeden, F., Troise, F.L., Todd, D.K., 1990. The Water Encyclopedia, second ed. Lewis, Boca Raton, FL.

Walker, N.D., 1996. Satellite assessment of Mississippi River plume variability: causes and predictability. Remote Sensing of the Environment 58 (1), 21–35.

Walker, N.D., Hammack, A.B., 2000. Impacts of winter storms on circulation and sediment transport: Atchafalaya–Vermilion Bay region, Louisiana, USA. Journal of Coastal Research 16 (4), 996–1010.

Wang, X.H., Pinardi, N., Malacic, V., 2007. Sediment transport and resuspension due to combined motion of wave and current in the northern Adriatic Sea during a Bora event in January 2001: a numerical modelling study. Continental Shelf Research 27 (5), 613–633.